

## 3D Additive Manufacturing for Alloy Tool Steel

M. TANO Y. MISADA T. NAGAHAMA T. MIZOGUCHI T. MITSUI H. HOSHINO

*Laser beam powder bed fusion (PBF-LB) for alloy tool steel is developed to fabricate casting dies for automobile parts by additive manufacturing. Internal defects such as pores, micro cracks and carbide, which deteriorate mechanical properties, have been improved by the developed process parameters, reduction of crack susceptibility index, and heat treatment. As a result, the workpieces manufactured using PBF-LB achieved a tensile strength and Charpy impact value equivalent to the wrought samples.*

**Key Words:** additive manufacturing, laser beam powder bed fusion, alloy tool steel

### 1. Introduction

Recently, 3D additive manufacturing (AM) technology has been drawing growing attention as an innovative production technology<sup>1)</sup>. Laser Beam Powder Bed Fusion (PBF-LB), one of the major methods in metal additive manufacturing, is capable of fabricating internal structures and complex shapes that cannot be achieved by conventional methods<sup>2)</sup>. One example of application is for the casting molds for automobile parts, where cooling paths with complex shapes inside are installed for optimizing the cooling conditions based on the shape, and this has enabled improved product dimensional accuracy and longer mold lifespans compared to ordinary molds<sup>3)-5)</sup>. The PBF-LB method, on the other hand, uses a laser to melt and solidify metal powder, and if the fabrication conditions and powder characteristics are not appropriate, defects will arise inside the built sample and its mechanical properties will be degraded. In particular, materials with a high carbon content are prone to cracking and are difficult to form. Therefore, when molds are processed by the PBF-LB method, maraging steel with high toughness is used, but it is inferior to the alloy tool steel used for ordinary casting molds in terms of performance characteristics such as thermal conductivity and thermal fatigue (heat check).

For this reason, this study aims to establish a foundation for 3D additive manufacturing technology of the SKD61 alloy tool steel that is used for casting molds. This paper presents the results of our investigation on the current status of PBF-LB for alloy tool steels, the issues that need to be addressed to improve the fabrication quality, the measures that were considered, and the results of our verification of the effects.

### 2. Assessing the Current Status of PBF-LB

#### 2.1 Forming Method

PBF-LB, one of the major AM technologies, is used primarily for fabricating metal products. **Figure 1** shows a schematic diagram of the PBF-LB process. The powder bed is formed by spreading metal powder on a base-plate using a recoater. In this process, the powder bed is repeatedly irradiated with a laser to melt and solidify the powder, and the layers are formed one by one. In this way, it is possible to fabricate internal structures and complex shapes by stacking and forming the shape of the product one layer at a time.

#### 2.2 Fabrication Experiment

The fabrication machine used was an SLM280<sup>HL</sup> manufactured by SLM Solutions (maximum fabrication dimensions: 280mm × 280mm × 350mm). SKD61 powder (grain size  $\phi$ 10 to 45  $\mu$ m) was used as the metal powder. **Table 1** shows the chemical composition. **Figure 2** shows the major fabrication parameters for the PBF-LB process. In the PBF-LB process, it has been reported that there is a correlation between the energy density  $E$  ( $J/mm^3$ ), which is a measure that encompasses these fabrication parameters, and the quality of the

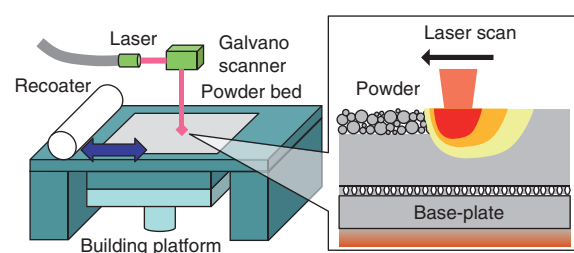


**Fig. 1** Schematic of PBF-LB

built sample<sup>6)</sup>. The energy density is expressed by the following equation where  $P$  is the laser power (W),  $v$  is the scan speed (mm/s),  $s$  is the hatching pitch (mm), and  $t$  is the layer thickness (mm).

$$E = P/vst \tag{1}$$

In this study, we also evaluate the fabrication results from the relationship between the energy density and the relative density, which is an evaluation index for the built sample's quality. **Table 2** shows the fabrication conditions. 16 specimens (15mm × 15mm × 30mm) with different fabrication parameters were fabricated on a base-plate, and the relative density to the theoretical density of 7.78 g/cm<sup>3</sup> was measured using Archimedes' principle. To reduce thermal stress by mitigating the temperature gradient in the built sample, the powder bed is preheated by a heater placed under the base-plate, and the temperature was set to 200°C for the fabrication conducted in this report.

**2. 3 Experiment Results**

**Figure 3** shows the relationship between the energy density and the relative density. This shows that, as the energy density increased, the relative density also increased, but once the energy density exceeded an appropriate level, the relative density decreased. Thus, high relative densities were obtained in the appropriate energy density range, with a maximum value of 99.5%. In the range where the energy density is not appropriate, we think that the relative density is low because the powder remains unmelted during laser irradiation and spatters, resulting in subpar melting, which left pores inside the built sample.

**Table 1** Chemical composition (wt%)

C	Si	Mn	P	S	Cr	Mo	V
0.41	1.09	0.42	0.012	0.006	5.02	1.25	1.10

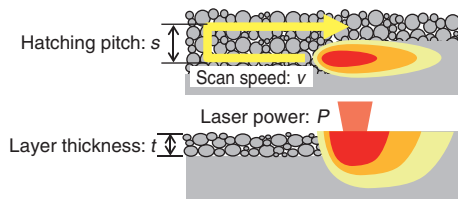


**Fig. 2** Process parameters

**Table 2** Fabrication conditions

Laser power	155 to 480 W
Scan speed	460 to 1 430mm/s
Hatching pitch	0.08 to 0.21mm
Layer thicknes	0.05mm

To evaluate the mechanical properties of the built samples, a tensile test (JIS Z 2241 compliant, specimen dimensions  $\phi 7\text{mm} \times 64\text{mm}$ ) of a specimen processed under conditions where a relative density of 99.5% was obtained and a Charpy impact test (JIS Z 2242 compliant, specimen dimensions 12mm × 12mm × 56mm) were conducted. The hardness of the as-built specimen was 55 HRC, and so the specimen was heat-treated at 600°C for 4 hours (air-cooled) two times to bring it to 47 HRC, which is the hardness required for casting molds (42 HRC to 52 HRC). **Figure 4** shows the results of the mechanical property measurements. The tensile strength and Charpy impact values of the specimens were found to be reduced by 80% and 20%, respectively, compared to the wrought sample. Since it was thought that defects inside the built sample may be a factor in the reduced mechanical properties, we observed cross-sections of the built sample and found micropores, microcracks, and precipitation of carbides as shown in **Fig. 5**.

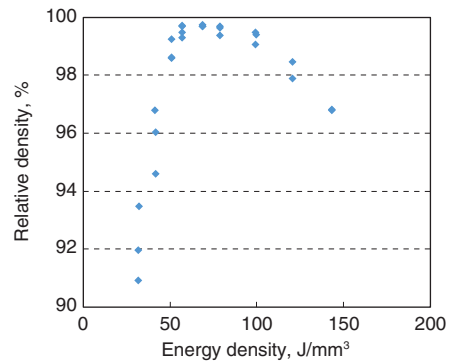


**Fig. 3** Relationship between energy density and relative density

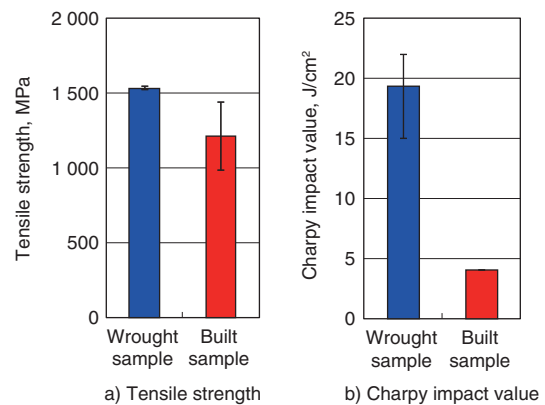


**Fig. 4** Measurement result of mechanical properties

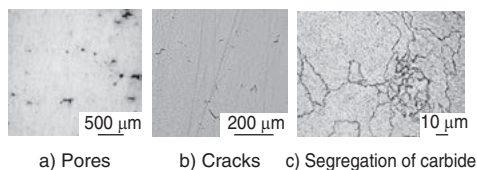


**Fig. 5** Optical micrograph of specimens

### 3. Improving Fabrication Quality

Micropores, microcracks, and precipitation of carbides were cited as factors reducing the mechanical properties of the built samples. To achieve the same mechanical properties as those of the wrought sample, we investigated measures to reduce internal defects and improve the fabrication quality.

#### 3.1 Porosity Reduction

The shape of the pores suggests that they are caused by poor fusion during laser irradiation, and so we investigated how to suppress the spatter that causes this. **Figure 6** shows the result of the thermal fluid analysis. The center of the molten pool is particularly hot and the evaporation pressure increases, which is thought to cause spattering. Therefore, the laser power must be reduced to suppress the over-heat input. However, the relative density is expected to decrease because the fabrication quality is correlated with the energy density. Therefore, noting that the laser power has a significant effect on the depth of the molten pool, the layer thickness was reduced to 0.03mm by taking into account the powder grain size. As a result, the relative density was improved to 99.8% using this method, compared with the 99.5% obtained under the conventional fabrication conditions.

#### 3.2 Suppression of Cracking

The cracks are thought to be caused by the opening of the thin liquid phase section remaining between the solid phases due to thermal stress during the solidification process of the molten pool. Therefore, in order to reduce the amount of low-melting-point compounds remaining in the liquid phase section, a high thermal conductivity

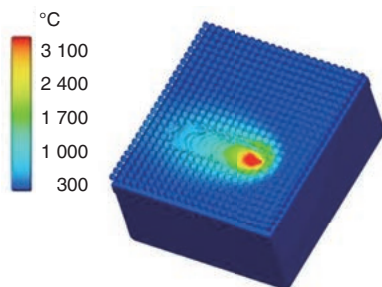


**Fig. 6** Result of thermal fluid analysis

material for molds (manufactured by Daido Steel, referred to as “high thermal conductivity material” below) was selected because it has a low high-temperature cracking susceptibility coefficient  $K$ , which is used as an index of cracking susceptibility in the field of welding, and is expected to suppress the occurrence of cracking. The high-temperature cracking susceptibility coefficient  $K$  is calculated from the content of each element by the following equation<sup>7)</sup>.

$$K = \frac{C \times \left[ S + P + \frac{Si}{25} + Ni/100 \right]}{3Mn + Cr + Mo + V} \times 100 \quad (2)$$

**Table 3** shows the chemical composition. Due to the low composition of carbon and silicon, the high-temperature crack susceptibility coefficient was reduced from the 2.9 of SKD61 to 0.7. While the conventional number of cracks was 26 per mm<sup>2</sup> in **Fig. 5** (b), no cracks were found within the observed range, indicating that cracks could be significantly suppressed (**Fig. 7**).

#### 3.3 Suppression of Carbide Segregation

Because the composition of the high thermal conductivity material is different from that of SKD61, we investigated the tempering temperature where a hardness in the mold usage range can be obtained. **Figure 8** shows the relationship between the tempering temperature and the hardness. A hardness within the mold usage range was obtained below 600°C. **Figure 9** shows the result of cross-sectional observation after tempering at 550°C. This confirms that the carbide precipitation observed in **Fig. 5** (c) was reduced.

#### 3.4 Evaluation of Mechanical Properties

To improve the fabrication quality, a combination of the suppression of over-heat input, reduction of the crack susceptibility coefficient, and the optimization of the tempering temperature were used in the fabrication experiments, and the mechanical properties were evaluated. Since the hardness of each specimen after tempering at 550°C was 50 HRC, it was compared with the

**Table 3** Chemical composition (wt%)

C	Si	Mn	P	S	Cr	Mo	V
0.32	0.06	0.37	0.008	0.007	5.21	1.22	0.40



**Fig. 7** Optical micrograph of specimens

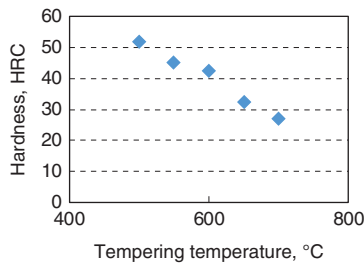


**Fig. 8** Relationship between tempering temperature and hardness

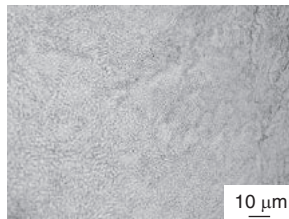


**Fig. 9** Optical micrograph of specimens

catalog value of SKD61 wrought sample with equivalent hardness<sup>8)</sup>. **Figure 10** shows the measurement results of the mechanical properties. Due to the improvements in the fabrication quality, it was confirmed that tensile strength and Charpy impact value equivalent to or higher than those of the SKD61 wrought sample could be obtained. In particular, we believe that the significant improvement in the Charpy impact value compared to the wrought sample is due to the finer metallurgical structure caused by rapid cooling solidification, which is a characteristic of the PBF-LB process.

#### 4. Conclusion

To realize future production technology innovations, we have established a foundation for additive manufacturing technology for alloy tool steel by the PBF-LB process. To resolve the issue of degradation of mechanical properties due to internal defects caused by heat treatment and melting and solidification during laser irradiation, measures to improve the fabrication quality were investigated, and mechanical properties equivalent to those of wrought samples were obtained.

Looking forward, we will evaluate prototype molds and develop optimal design technology for utilizing PBF-LB, and we aim to bring about production technology innovations through practical applications of this technology.

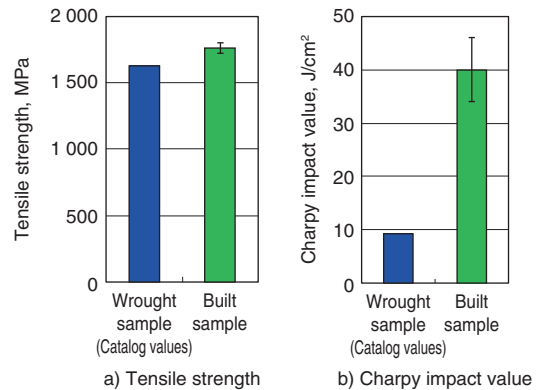


**Fig. 10** Measurement result of mechanical properties

#### References

- 1) H. KYOGOKU: Recent Trend on Laser Metal Additive Manufacturing, *Journal of Japan Society for Precision Engineering*, Vol. 82, No. 7 (2016) 619-623 (in Japanese).
- 2) Technology Research Association for Future Additive Manufacturing (TRAFAM): *Kinzoku Sekisou Zoukei Gijutsu Nyumon* (2016) 8 (in Japanese).
- 3) H. KYOGOKU: Progress in Laser Additive Manufacturing Technology of Metals, *Journal of the Japan Welding Society*, Vol. 83, No. 4 (2014) 250-253 (in Japanese).
- 4) M. Mazur, M. Leary, M. McMillan, J. Elambasseril, M. Brandt: SLM additive manufacture of H13 tool steel with conformal cooling and structural lattices, *Rapid Prototyping Journal*, Vol. 22, No. 3 (2016) 504-518.
- 5) M. Mazur, P. Brincat, M. Leary, M. Brandt: Numerical and experimental evaluation of a conformally cooled H13 steel injection mould manufactured with selective laser melting, *Int. J. Advanced Manufacturing Technology*, Vol. 93 (2017) 881-900.
- 6) T. KIMURA, T. NAKAMOTO: Microstructures and Mechanical Properties of Al-10% Si-0.4% Mg Fabricated by Selective Laser Melting, *Journal of Japan Society of Powder and Powder Metallurgy*, Vol. 61, No. 11 (2014) 531-537 (in Japanese).
- 7) F. MATSUDA: Yousetsuware ni kansuru Zairyoushou no Shomondai -Gyokoware ni tsuite-, *Journal of the Japan Welding Society*, Vol. 44, No. 7 (1975) 546-551 (in Japanese).
- 8) Daido Steel Co., Ltd: DHA1-A Catalog No. SS0901 (in Japanese).



M. TANO \*



Y. MISADA \*\*



T. NAGAHAMA \*\*\*



T. MIZOGUCHI \*\*\*\*



T. MITSUI \*\*\*\*



H. HOSHINO \*\*\*\*\*

\* *Innovative Processing R&D Dept., Research & Development Division, Dr. Eng.*

\*\* *Material R&D Dept., Research & Development Division*

\*\*\* *BR Marketing Dept., Sales & Marketing Division*

\*\*\*\* *Innovative Processing R&D Dept., Research & Development Division*

\*\*\*\*\* *Materials Innovation Engineering Dept., Production Engineering Division*